End effect of corroded steel bar in concrete specimen during corrosion test by galvanostatic method

Peng Zhao, Gang Xu, Qing Wang, and Xuan Wang
Hubei Key Laboratory of Disaster Prevention and Mitigation, China Three Gorges University

College of Civil Engineering& Architecture, China Three Gorges University

ABSTRACT

The galvanostatic method is a commonly used accelerated corrosion method in studying the durability of concrete structures caused by steel corrosion. If this method is not adequately controlled, the ends of steel bars will be corroded seriously (this phenomenon is called end effect), which is not common in natural corrosion. How to effectively control the end effect during electrified corrosion is helpful to make the characteristics of electrified corrosion more similar to that of natural corrosion. In this paper, experimental and electromagnetic numerical simulation methods are used to study the influence of cathode and corrosion medium coverage area along the longitudinal direction on the end effect of steel bar before producing corrosion crack. The results showed that the wider the coverage area of the corrosive medium (NaCl solution with a mass concentration of 3%), the longer the corrosion area of reinforcement along the longitudinal direction, the more prone the end effect is. The change of cathode length has no noticeable effect on the corrosion area of reinforcement along the longitudinal direction when the corrosion medium coverage area is constant. Increasing the distance between the end of the corrosion medium coverage area and the end of the reinforcement can effectively avoid the end effect.

1. INTRODUCTION

Steel bar corrosion is the overriding factor leading to the insufficient durability of reinforced concrete structures (RCSs), which will seriously endanger the safety and service life of RCSs [1]. Among the indicators characterizing the corrosion characteristics of steel bars in concrete, the corrosion area of steel bars is particularly important. Different corroded areas will lead to different distributions of corroded expansion force, which will affect the bonding performance and the bearing capacity of components [2].

Due to the slow corrosion process in the natural environment, it takes much time for steel bars in concrete to corrode to a certain extent [3-5], which many researchers cannot accept. In order to quickly obtain corroded concrete members, most scholars use the accelerated corrosion method, including the use of galvanostatic method [6-11], cyclic wetting and drying [12-13], artificial climate environment [14], among which the galvanostatic method is the most widely used. However, due to the lack of relevant test standards, the setting of corrosion methods is diverse, making it difficult to control the corrosion area of reinforcement accurately. The essence of electrifying corrosion of steel bars in concrete is the reaction of the electrolytic cell, and the corrosion of the buried electrodes in the power system is also caused by the reaction of the electrolytic cell. It has been pointed out that the corrosion of the buried linear electrode is not uniform, and the end is severely corroded, the middle part is relatively slightly corroded, and this phenomenon is called end effect [15-16]. The end effect may also exist when the corroded RC specimen is obtained by galvanostatic method, which may weaken the anchorage performance of the steel bar and affect the mechanical properties of concrete members. Therefore, it is necessary to study the influencing factors of end effect and its avoidance methods during electrifying corrosion.

Among the influencing factors of electrifying corrosion, the longitudinal setting area of corrosion medium and cathode length may be important influencing factors of end effect. In the existing studies, for the corrosive medium, some literature only set the corrosive medium in the local area of the specimen [17-19], while others set the corrosive medium along the full length of the specimen [20-22]. For the length of the cathode along the longitudinal direction, when the corrosion medium coverage area on large-scale concrete members is wide, the cathode length in some literature is minimal [21], while the cathode length in some literature is large [22-23]. Unfortunately, there are few studies on the influence of corrosion medium setting area and cathode size on reinforcement corrosion area. G. Xu et al.[19,24] pointed out that

the corrosion area of the steel bars along the ring direction is mainly the area facing the cathode side. The corrosion form of the steel bars is significantly affected by the location of the cathode and the salt solution immersion area. C.-Q. Fu et al. [25-27] have similar findings. It is a pity that the end effect of steel corrosion is rarely mentioned in the existing literature when RC is corroded by galvanostatic method.

In order to explore the control method of end effect when RC specimens are corroded by galvanostatic method, it is necessary to study the influence mechanism of the longitudinal coverage area of corrosion medium and the length of cathode on the end effect. For this purpose, we try to use experimental and numerical simulation methods to study this problem. On this basis, the influence law of the cathode and corrosion medium arrangements on the end effect will be clarified to provide a reference to avoid the appearance of such corrosion phenomenon.

2. ELECTRIFIED CORROSION TEST

2.1. Experimental program

2.1.1. Specimen preparation

In this test, a total of 6 RC specimens with a size of 100mm × 100mm × 400mm were designed and fabricated, and each specimen was equipped with a diameter of 14mm HPB300 steel bars, as shown in Figure 1. The concrete strength grade of all the specimens was C30, and the composition of the concrete mix was 0.520(Water) : 1 (Cement) : 1.709 (Fine aggregate) : 3.173 (Coarse aggregate), in which the cement was of Huaxin brand P•O42.5 Ordinary Portland Cement (made in China), the coarse aggregate was continuous grading macadam with a particle size of 5–20 mm, the fine aggregate was the river sand with a fineness modulus of 3.3 and the water was tap water. After 28 days of standard curing, the concrete compressive strength under standard test conditions was 35.6Mpa. Before concrete casting, the reinforcement was treated according to standard [28] to ensure no corrosion on the surface of steel bars. In order to facilitate the positioning of the steel bars during the casting of specimens, rubber sleeves with a length of 12 mm were set at both ends of the steel bars.
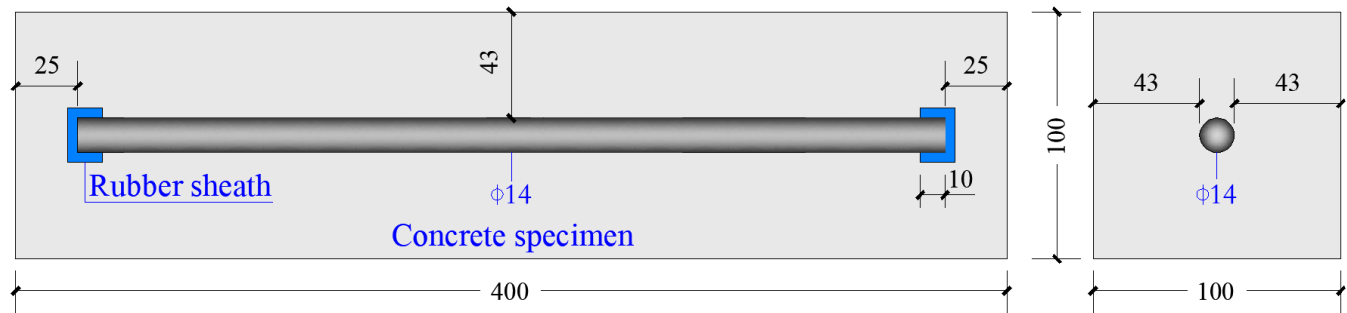

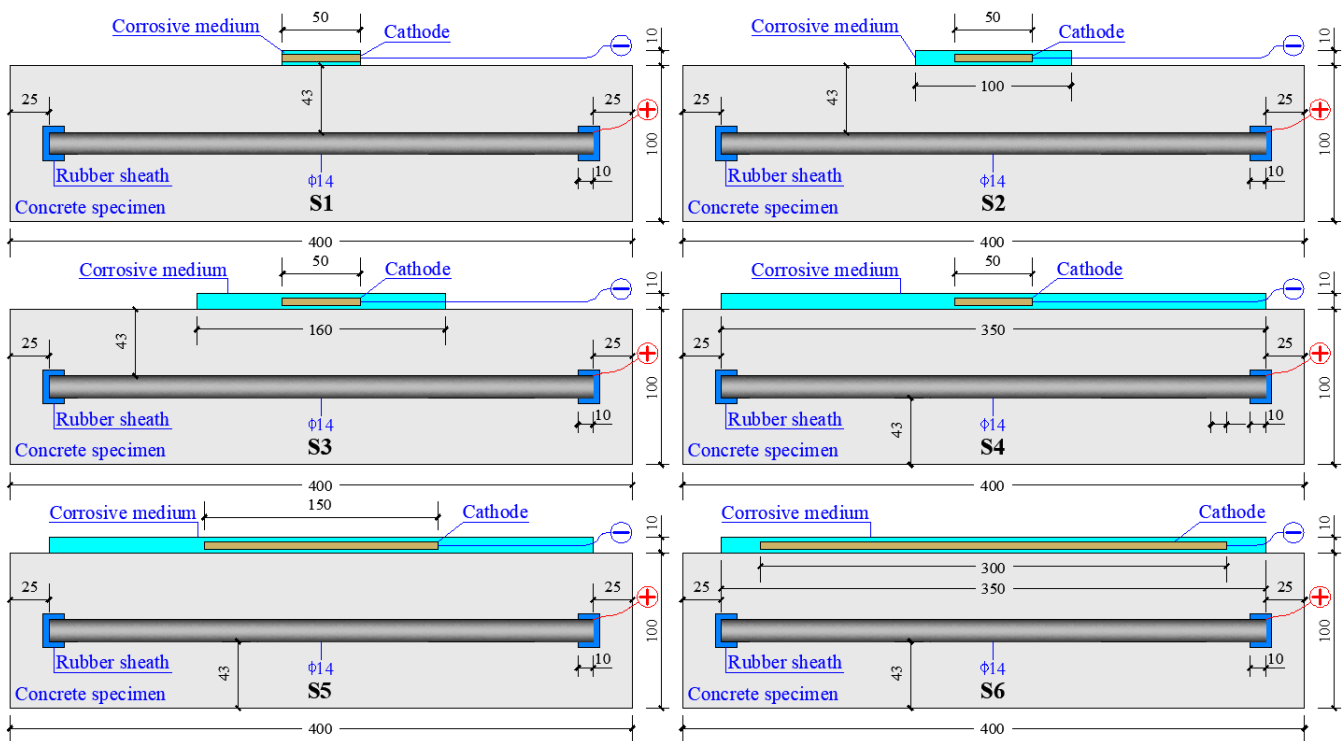**Figure 1.** The size and reinforcement of specimen (unit: mm)

Figure 2. Corrosion condition (unit: mm)

2.1.2. Corrosion scheme

In order to clarify the influence of cathode length and corrosion medium cover length on the longitudinal corrosion area of steel bars, six corrosion conditions were designed. The size of the cathode, cofferdam and its specific location are shown in Figure 2. Before the beginning of electrifying corrosion, the test specimens were immersed in NaCl solution with a mass concentration of 3% for 14 days. Then the NaCl solution was injected into the cofferdam as the corrosive medium, and a 304 stainless steel sheet with a thickness of 2mm was set as the cathode. During the corrosion period, the energizing current is 102mA, equal to the product of the preset current density 0.002 mA / mm^2 and the surface area of the exposed section of the steel bar (the current density is determined according to reference [29]). In order to stabilize the temperature and humidity of the specimen, a layer of preservative film was covered on its surface, and the temperature of the corrosion environment was controlled at 20 ± 2 °C. In order to facilitate comparison with the simulation results, all specimens were charged only before concrete corrosion cracking, and the charging time was 12 h. After the corrosion was finished, the specimen will be broken, the residual mortar on the surface of the steel bar will be cleaned, and the corrosion area of the steel bar will be recorded.

2.2. Experimental results

The corrosion of reinforcement ends in each test specimen is shown in Figure 3. When the cathode length is constant (such as S1, S2, S3, and S4 specimens), the longitudinal corrosion area of reinforcement increases with the increase of corrosion medium coverage area along the longitudinal direction of specimen. However, when the coverage area of corrosion medium along the longitudinal direction is different, the main corrosion areas of reinforcement are obviously different. When the corrosion medium does not cover the end of steel bars (such as S1, S2, and S3 specimens), the corrosion area of the reinforcement is mainly concentrated in the area covered by the corrosion medium, the surface of the reinforcement adjacent to the corrosion medium is also slightly rusted, and the end of the reinforcement is almost not rusted, that is, the end effect is not obvious. When the end of the reinforcement is covered with corrosive medium (such as S4 specimen), the most severely corroded area is concentrated in the reinforcement at the edge of the rubber sleeve (as shown in the frame selected part in Figure 3), that is, the end effect is significant. When the corrosion medium coverage area is constant (such as S4, S5, and S6 specimens, the corrosion medium covers the end of the reinforcement), there is no significant difference in the corrosion area of the reinforcement along the longitudinal direction in each specimen with the increase of the cathode length. The most serious corrosion area of reinforcement is concentrated in the reinforcement at the edge of rubber sleeve, and the end effect is significant. It can be concluded that the longitudinal coverage area of the corrosive

3

medium along the specimen is the key to affecting the longitudinal corrosion area and end effect of reinforcement, while the cathode length is not obvious. In order to further clarify the influence of the longitudinal coverage area of the corrosive medium and the cathode length on the end effect, the electromagnetic numerical simulation method will be used for further analysis.
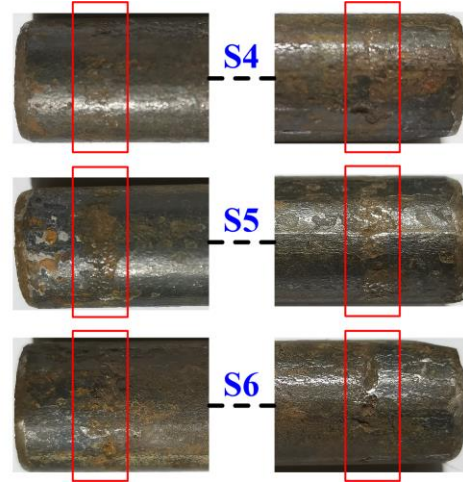

Figure 3. Corrosion of steel bar ends in each specimen

3. NUMERICAL SIMULATION

The principle of electrified corrosion is electrolytic cell reaction, and the amount of steel corrosion is the amount of electrolysis of iron matrix. When controlling the corrosion amount of reinforcement, it is often calculated based on Faraday's Electrolysis law through the energizing current value and power supply time, as shown in formula (1). Among them, the energizing current can be expressed by the product of the current density and surface area, i.e., formula (2). If the current density distribution on the surface of the steel bar during energizing corrosion period can be clarified, the corrosion on the surface of the steel bar can be known. From the perspective of electromagnetics, energized corrosion is a process of current conduction, which flows from the positive pole of the power supply and flows into the negative pole. In the study of the current conduction problem, a numerical simulation method based on electromagnetic theory is often used to simulate the surface current density distribution of related components [30-31]. Therefore, for the problem of electrified corrosion of reinforcement in concrete specimens, an electromagnetic model can be tried to build by measuring the electrical parameters (including resistivity and dielectric constant) of reinforcement, concrete, corrosive medium, cathode, and other materials, and simulate the current density distribution on the reinforcement surface, so as to obtain the corrosion condition of reinforcement surface.

$$\square m_{\mathrm{F}} = \frac{I \cdot M \cdot t}{n \cdot F} \quad (1)$$

$$I = \iint_{S} J(x, y, z) dS \quad (2)$$

In formula (1), $\triangle m_{\mathrm{F}}$ is the theoretical corrosion amount calculated by *Faraday's* law, I is the energizing current, n is the number of valence electrons lost during the oxidation of the iron matrix, and its value is 2; F is the Faraday constant, its value is 96485C/mol; M is the atomic weight of iron with a value of 56g/mol; t is power on time. In formula (2), $J(x,y,z)$ is the current density of a certain micro-element.

3.1. Finite element model

In this paper, the simulation calculation is carried out by using the finite element software ANSYS multiphysics. The simulation conditions and model dimensions are consistent with the test (see Figure 2 and Table 1 for details), and the schematic diagram of the model is shown in Figure 4. When dividing the grid, the grid size of the steel bar is 1mm, the size of rubber sleeve, mortar, cathode, and salt solution is 5mm, and the air is 10mm. Each grid type is a three-dimensional tetrahedral element, which is a free grid division, and the element types are all solid 231 units. When applying load and restraint, couple the potentials of all nodes on the steel bar, and input a current of 102mA to the middle node of the steel bars; couple the potentials of all the nodes of the cathode and set the potential to 0; set the potentials of all the nodes on the outermost layer of the air domain to 0. The main parameters involved in the five materials in the model are resistivity and relative permittivity. Among them, the concrete resistivity is measured after 14 days of soaking the specimens poured in the same batch as in the experiment. The

specific values of resistivity and relative permittivity of each material are shown in Table 2.
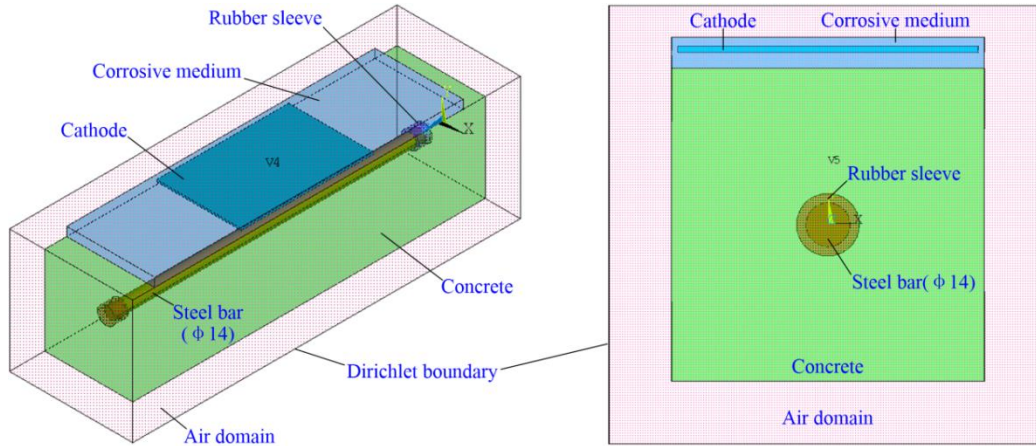

Figure 4. Simulation model (taking S5 specimen as an example)

Table 2. Parameters of simulation model

Parameter category	Concrete	Steel bar/304 stainless steel	Air	3% NaCl solution	Rubber
Resistivity ($\Omega \cdot m$)	33	9.78×10^{-8}	1×10^{13}	0.25	1×10^{13}
Relative permittivity	12	10^{-7}	1.006	81.5	2.5

Note: The resistivity of NaCl solution with a mass concentration of 3% was measured at 20 °C.

3.2. Simulation results and analysis

The current density distribution on the reinforcement surface under various working conditions is shown in Figure 5. When the cathode length is constant, the current density distribution area on the reinforcement surface along the longitudinal direction is mainly concentrated in the corrosion medium coverage area. With the increase of the corrosion medium coverage area along the longitudinal direction, the current density on the reinforcement surface at the edge of the rubber sleeve gradually increases, the end effect gradually appears. When the corrosive medium covers the end of the steel bar, the end effect is most obvious, where the current density is the largest. However, when the corrosion medium covers the end of reinforcement, the increase of cathode length has no obvious effect on the current density distribution on the reinforcement surface. Obviously, the influence of the corrosion medium coverage area along the longitudinal direction and the cathode length on the distribution area of main current density along the longitudinal direction of reinforcement surface is consistent with that on the longitudinal corrosion area of reinforcement in the test, which shows that the corrosion area on reinforcement surface before concrete corrosion cracking can be predicted by using the numerical simulation method based on electromagnetism.
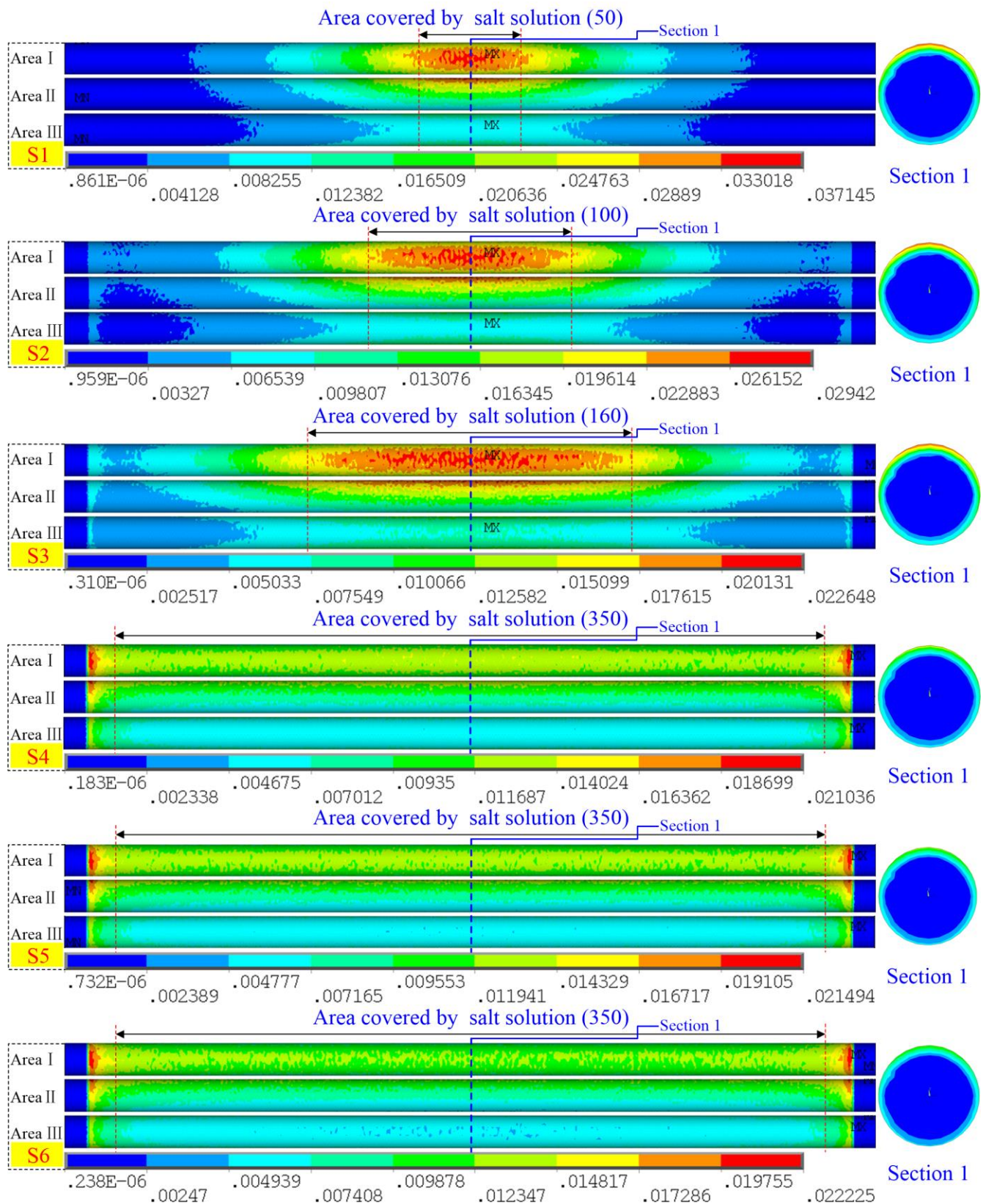
Figure 5. Current density distribution on reinforcement surface of each specimen
(Area I denotes top view; Area II denotes side view; Area III denotes bottom view)
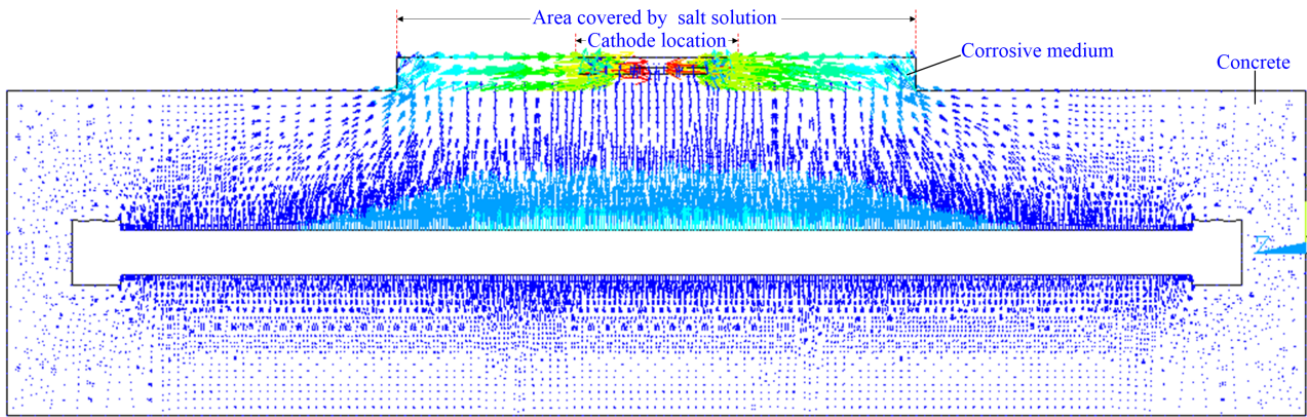
Figure 6. The current flow direction of the S3 specimen along the longitudinal middle section

4. DISCUSSION

In conclusion, the longitudinal coverage of corrosive media is the critical factor affecting the longitudinal corrosion area and end effect of reinforcement. The analysis shows that this is because the coverage of the corrosive medium changes the current path flowing from the surface of the distal steel bar to the cathode. When the potential between the steel bar and the cathode is the same, the current tends to flow from the path with less resistance to the cathode. In this test, the resistivity of the corrosive medium is much lower than that of concrete. When the covering length of the corrosive medium is small, the current on the far-end reinforcement surface flows to the cathode through concrete. However, because of the high resistivity of concrete, the resistance of the current path is considerable, which results in the current density on the distal reinforcement surface being small. Although there is an overflow at the end of reinforcement, the large concrete resistance makes the end effect difficult to occur. When the coverage of the corrosive medium increases, the current path from the surface of distal reinforcement to the cathode will change, as shown in Figure 6, the current will first flow into the nearest corrosive medium and then be transmitted to the cathode through the corrosive medium, resulting in a certain current density distribution on the surface of the distal reinforcement. With the increase of corrosion medium coverage area along the longitudinal direction, the more serious the corrosion of the distal reinforcement is, the more obvious the end effect is. In addition, the cathode length only changes the resistance of current conduction from the end of the corrosion medium coverage area to the end of the cathode, but because the resistivity of the corrosion medium is small, this resistance is also very small and can be ignored. Therefore, when the corrosion medium coverage area remains unchanged, the change of cathode length has no

obvious effect on the corrosion area of reinforcement along longitudinal direction, and the reinforcement in the area covered by corrosive medium will be rusted. It can be concluded that controlling the longitudinal coverage area of the corrosion medium along the specimen is the key to controlling the end effect. Increasing the distance between the end of the corrosion medium coverage area and the end of the reinforcement can effectively avoid the end effect.

5. CONCLUSION

Based on the experimental work and numerical simulation of galvanostatic accelerated corrosion of steel bar in mortar, the following conclusions can be drawn:
(1) When the resistivity of corrosive medium is much lower than that of concrete, the longitudinal coverage area along the specimen is the key to affecting the corrosion area of reinforcement, and the wider the coverage area, the wider the corrosion area of reinforcement along the longitudinal direction, the more prone the end effect is. When the corrosion medium coverage area is constant, the change of cathode length has no obvious effect on the corrosion area of reinforcement along the longitudinal direction.
(2) The numerical simulation method based on electromagnetism can be used to predict the corrosion area of reinforcement before corrosion crack.
(3) Increasing the distance between the end of the corrosion medium coverage area and the end of the reinforcement can effectively avoid the end effect.

REFERENCES

1. Mehta. P.K.,1991. Concrete durability - fifty years progress, Proc. of 2nd Inter. Conf. On Concrete Durability. ACISP. J. 126(1):1-31.

2. Fares Jnaid, Riyad S. Aboutaha, 2016. Residual flexural strength of corroded reinforced concrete beams. Engineering Structures, 119: 198–216.

3. K. Asami, M. Kikuchi, 2003. In-depth distribution of rusts on a plain carbon steel and weathering steels exposed to coastal–industrial atmosphere for 17 years. Corrosion Science, 45: 2671-2688.

4. Chuanqing Fu, Nanguo Jin, Hailong Ye, et al., 2017. Corrosion characteristics of a 4-year naturally corroded reinforced concrete beam with load-induced transverse cracks. Corrosion Science, 117: 11-23.

5. Amry Dasar, Hidenori Hamada, Yasutaka Sagawa, et al., 2017. Deterioration progress and performance reduction of 40-year-old reinforced concrete beams in natural corrosion environments. Construction and Building Materials, 149.

6. Yingang Du, Martin Cullen, Cankang Li, 2013. Structural effects of simultaneous loading and reinforcement corrosion on performance of concrete beams. Construction and Building Materials, 39: 148-152.

7. Jianfeng Dong, Yuxi Zhao, Kun Wang, et al., 2017. Crack propagation and flexural behaviour of RC beams under simultaneous sustained loading and steel corrosion. Construction and Building Materials, 151: 208-219.

8. Y.X. Zhao, Y.Z. Wang, J.F. Dong, 2021. Prediction of corrosion-induced concrete cracking under external loading and stirrup constraint. Construction and Building Materials, 266: 121053

9. Goitseone Malumbela , Pilate Moyo, Mark Alexander, 2009. Behaviour of RC beams corroded under sustained service loads. Construction and Building Materials, 23: 3346-3351.

10. Roberto Capozucca, 2008. Detection of damage due to corrosion in prestressed RC beams by static and dynamic tests. Construction and Building Materials, 22: 738-746

11. Hedong Li, Bo Li, Ruoyu Jin, et al., 2018. Effects of sustained loading and corrosion on the performance of reinforced concrete beams. Construction and Building Materials, 169: 179-187.

12. Xiao-Hui Wang, Yang Gao, 2016. Corrosion behavior of epoxy-coated reinforced bars in RC test specimens subjected to pre-exposure loading and wetting-drying cycles. Construction and Building Materials, 119: 185-205.

13. Je-Kyoung Kim, Seong-Hoon Kee, Cybelle M. Futalan, Jurng-Jae Yee, 2020. Corrosion monitoring of reinforced steel embedded in cement mortar under wet-and-dry cycles by electrochemical impedance spectroscopy. Sensors, 20, 199.

14. Kuang-Yu Dai, Chang Liu, Da-Gang Lu, Xiao-Hui Yu, 2020. Experimental investigation on seismic behavior of corroded RC columns under artificial

climate environment and electrochemical chloride extraction: A comparative study. Construction and Building Materials, 242: 118014.

15. Tong Xuefang, Zheng Zhihui, Tan Bo, Lu Hailiang, et al., 2018. Corrosion Rate Simulation and Influence Factors of a Vertical DC Grounding Electrode. IEEE Access, 6: 57230-57238.

16. Yun Teng, Xishan Wen, Hansheng Cai, Lei Jia, et al., 2019. Analysis on structural parameters and electrical performance of dc deep well grounding electrode. The Journal of Engineering, 16: 2366-2370.

17. Goitseone Malumbela , Pilate Moyo, Mark Alexander, 2009. Behaviour of RC beams corroded under sustained service loads. Construction and Building Materials, 23: 3346-3351.

18. Huafu Pei, Zongjin Li, Jinrui Zhang, Qian Wang, 2015. Performance investigations of reinforced magnesium phosphate concrete beams under accelerated corrosion conditions by multi techniques. Construction and Building Materials, 93: 989-994.

19. Peng Zhao, Gang Xu, Qing Wang, Guangjie Tang, 2019. Influence of sustained load on corrosion characteristics of reinforced concrete beams under galvanostatic accelerated corrosion. Construction and Building Materials, 215: 30-42.

20. Yingshu Yuan, Yongsheng Ji, Surendra P. Shah, 2007. Comparison of two accelerated corrosion techniques for concrete structures. ACI Structural Journal, 104(3): 344-347.

21. Hailong Ye, Chuanqing Fu, Nanguo Jin, Xianyu Jin, 2018. Performance of reinforced concrete beams corroded under sustained service loads: A comparative study of two accelerated corrosion techniques. Construction and Building Materials, 162: 286-297.

22. Ballim Y, Reid JC., 2003. Reinforcement corrosion and deflection of RC beams-an experimental critique of current test methods. Cement and concrete composites, 25:625-632.

23. Ali Siad, Mohamed Bencheikh, Luaay Hussein, 2017. Effect of combined pre-cracking and corrosion on the method of repair of concrete beams. Construction and Building Materials, 132: 462-469.

24. Gang Xu, Rui Zhang, Yanzhou Peng, Lili Xu, 2017. Study on influence of corroded characteristics of reinforcing bars under galvanostatic accelerated corrosion before concrete cover cracking. J. Huazhong Univ. of Sci. & Tech. (Natural Science Edition), 45(3): 127-132.

25. Chuanqing Fu, Nanguo Jin, Hailong Ye, Jiamin Liu, Xianyu Jin, 2018. Non-uniform corrosion of steel in mortar induced by impressed current method: An experimental and numerical

investigation. Construction and Building Materials, 183: 429438.

26. Nan-guo Jin, Jia-hao He, Chuan-qing Fu, Xian-yu Jin, 2020. Study on experimental method and morphology of accelerated non-uniform corrosion of steel bars. Jour. of Zhejiang Univ. (Engineering Science), 54(03):483-490.

27. Jinwei Chen, Chuanqing Fu, Hailong Ye, Xianyu Jin, 2020. Corrosion of steel embedded in mortar and concrete under different electrolytic accelerated corrosion methods. Construction and Building Materials, 241: 117971.

28. National Standard of the People's Republic of China, 2002. GB/T50081-2002 Standard for Test Method of Mechanical Properties on Ordinary Concrete. China Architecture and Building Press, Beijing.

29. Maaddawy TAE, Soudki K, 2003. Effectiveness of impressed current technique to simulate corrosion of steel reinforcement in concrete. Journal of materials in civil engineering, 15(1): 41-47.

30. C.T.J. Low, E.P.L. Roberts, F.C. Walsh, 2007. Numerical simulation of the current, potential and concentration distributions along the cathode of a rotating cylinder Hull cell. Electrochimica Acta, 52(11): 3831–3840.

31. Chenglian Ma, Shujian Zhao, Li Sun, Letian Wang,et al.,2018. THE simulation study of DC grounding electrode based on CDEGS and ANSYS. Journal of Physics: Conference Series, 1072.1: 012006-012006.

•Corresponding author. E-mail address: postxg@163.com